# Visible-light photocatalytic $H_2$ evolution over a series of transition metal substituted Keggin-structure heteropoly blues

WANG ZhenLi, LU Ying*, LI YangGuang, WANG ShiMing & WANG EnBo*

*Key Laboratory of Polyoxometalate Science of Ministry of Education, Department of Chemistry, Northeast Normal University, Changchun 130024, China*

The visible light photocatalytic $H_2$ evolution activities of a series of transition-metal substituted Keggin-structure heteropoly blues $K_6SiW_{11}O_{39}M(H_2O) \cdot nH_2O$ (M = Co, Ni, Cu and Zn) were systematically studied with Pt nanoparticles as co-catalyst. The $H_2$ evolution rates were 150, 98, 65 and 48 $\mu$mol $h^{-1}g^{-1}$ for $SiW_{11}Cu$, $SiW_{11}Ni$, $SiW_{11}Co$ and $SiW_{11}Zn$, respectively, meaning that the order of photocatalytic activity of these heteropoly blues from transition-metal substituted polyoxometalates was: $SiW_{11}Cu >$ $SiW_{11}Ni > SiW_{11}Co > SiW_{11}Zn$. The catalysts could be efficiently reused for at least 5 cycles.

Citation: Wang Z L, Lu Y, Li Y G, et al. Visible-light photocatalytic $H_2$ evolution over a series of transition metal substituted Keggin-structure heteropoly blues. Chin Sci Bull, 2012, 57: 2265–2268, doi: 10.1007/s11434-012-5050-1

Photocatalytic $H_2$ evolution on a large scale from renewable solar energy using low cost catalysts has attracted much attention as an important aspect of sustainable energy production [1]. Homogeneous and heterogeneous photocatalysts have played an important role in photochemical conversion processes. Semiconductor materials including metal oxides, metal (oxy) sulfides and metal (oxy) nitrides have been widely studied as heterogeneous photocatalysts for water splitting [2–4]. Although homogeneous catalyst systems based on the first-row transition metals for photochemical hydrogen production were scarcely reported before 2000 [5–8], recently, non-precious metal-based homogenous catalysts have attracted continuously growing attention [9–14]. A more complex class of catalysts is the polyoxometalates (POMs). POMs are well-defined metal-oxygen clusters, which have drawn considerable interest because of their unique structural characteristics and their potential applications in catalysis, medicinal chemistry and nanotechnology [15]. With diverse and tunable structures, POMs can act as acid, redox, bifunctional (acid and redox) and

photo catalysts participating in many reactions. Recently, the photocatalytic $H_2$ evolution activity of some iso/hetero-polyoxotungstates (such as $[W_{10}O_{32}]^{4-}$ and $XW_{12}O_{40}^{n-}$ (X = Si, P, B, Ge, Fe, Co or $H_2$)) have been studied with Pt nanoparticles as co-catalyst and methanol as sacrificial agent [16–21]. However, most reported POM photocatalysts are only active under UV irradiation. There is high demand for POM photocatalysts with visible-light activity for more efficient use of solar energy.

In our search for POM photocatalysts with visible-light activity for photocatalytic $H_2$ evolution, we studied visible-light photocatalytic $H_2$ evolution over a series of heteropoly blues (HPBs) of transition metal substituted POMs (TMSPs) based on the following considerations. Firstly, transition metal ions can be substituted for one or more addenda atoms of POMs to form transition metal substituted polyoxometalates (TMSPs). The electronic structure of TMSPs can be adjusted through changing the transition metal ions participating in the substitution [22]. To our knowledge, the visible-light photocatalytic $H_2$ evolution behaviors of TMSPs have not been explored until now. Secondly, in the presence of a reducing agent, POMs could yield poly blues (PB) or

*Corresponding authors (email: wangeb889@nenu.edu.cn; luy968@nenu.edu.cn)

heteropoly blues (HPB) through the trapping of $d^1$ electrons at appropriate metal sites. HPB possesses adsorption in the visible light region (400–800 nm), which results from d–d and/or intervalence charge-transfer band excitation [23]. Recently, the photo-activity of HPB under visible light has attracted much attention, and HPBs have shown visible-light photocatalytic activity in some reactions [24–26].

# 1 Experimental

## 1.1 Material and methods

Unless otherwise stated, all chemicals used were analytical grade, commercially available and used without further purification. K-analysis was performed using a SpectrAA 220Z atomic absorption spectrometer (Varian). Si, W, Co, Ni, Cu and Zn were analyzed on a PLASMA-SPEC (I) ICP atomic emission spectrometer (Leeman). FT-IR spectra of the samples were recorded in the range of 400–4000 cm$^{-1}$ on an Alpha Centaurt FT/IR spectrophotometer using KBr pellets. The UV-Visible spectrum was recorded at ambient temperature on a SP-752PC Spectrophotometer using the 10 mm quartz cell. GC analyses were performed on GC-7890T instrument with a thermal conductivity detector and a 5 Å molecular sieve column (2 mm × 2 m) using $N_2$ as carrying gas.

## 1.2 Syntheses

$K_6SiW_{11}O_{39}Ni(H_2O) \cdot 15H_2O$, $K_6SiW_{11}O_{39}Co(H_2O) \cdot 14H_2O$, $K_6SiW_{11}O_{39}Cu(H_2O) \cdot 14H_2O$ and $K_6SiW_{11}O_{39}Zn (H_2O) \cdot 15H_2O$ (abbreviated $SiW_{11}Ni$, $SiW_{11}Co$, $SiW_{11}Cu$ and $SiW_{11}Zn$) were synthesized by the procedure reported in ref. [27]. Anal. Calcd. for $K_6SiW_{11}O_{39}Ni(H_2O)(H_2O) \cdot 15H_2O$ (%): K, 7.18; Si, 0.86; Ni, 1.81; W, 62.1; $H_2O$, 8.84. Found (%): K, 7.18; Si, 0.84; Ni, 1.78; W, 61.9; $H_2O$, 8.84. IR spectrum (KBr, cm$^{-1}$): 1003, 960, 904, 794, 675, 535. Anal. Calcd. for $K_6SiW_{11}O_{39}Co(H_2O) \cdot 14H_2O$ (%): K, 7.24; Si, 0.86; Co, 1.78; W, 62.53; $H_2O$, 8.37. Found (%): K, 7.24; Si, 0.83; Co, 1.82; W, 62.45; $H_2O$, 8.34. IR spectrum (KBr, cm$^{-1}$): 1001, 950, 907, 794, 689, 526. Anal. Calcd. for $K_6SiW_{11}O_{39}Cu(H_2O)$ $(H_2O) \cdot 14H_2O$ (%): K, 7.21; Si, 0.86; Cu, 1.97; W, 62.39; $H_2O$, 8.32. Found (%): K, 7.20; Si, 0.85; Cu, 1.93; W, 62.30; $H_2O$, 8.36. IR spectrum (KBr, cm$^{-1}$): 998, 959, 901, 793, 695, 536. Anal. Calcd. for $K_6SiW_{11}O_{39}Zn(H_2O) \cdot 15H_2O$ (%): K, 7.17; Si, 0.86; Zn, 2.00; W, 62.03; $H_2O$, 8.83. Found (%): K, 7.17; Si, 0.85; Zn, 2.02; W, 62.00; $H_2O$, 8.84. IR spectrum (KBr, cm$^{-1}$): 953, 906, 880, 801, 743, 537, 417.

## 1.3 Photocatalytic reaction

The photocatalytic reaction was carried out in a Pyrex inner-irradiation-type reaction vessel with magnetic stirring at room temperature. The photocatalytic reactions were performed in 50 mL distilled water containing $6 \times 10^{-5}$ mol/L TMSPs and 2.4 μmol/L Pt nanoparticles. Before the photocatalytic reaction, 0.1 g zinc powder was added to the reaction mixture as a reducing agent, concurrently, nitrogen gas was bubbled through the reaction mixture for 1 h to remove air and hydrogen. The mixture was then irradiated using a Xe lamp (500 W) with a Pyrex-glass filter ($\lambda > 400$ nm). The $H_2$ produced was analyzed using a GC 7890T instrument.

# 2 Result and discussion

After the addition of reducing agent (zinc powders), the color of the solutions changes to dark blue. The formation of HPBs has been confirmed by visible adsorption spectra (Figure S1), and the visible spectra of the reactant solutions exhibit obvious changes, which include a shift in the maximum adsorption and an increase of adsorption intensity (Figure S2).

Under visible light irradiation, $H_2$ is continuously produced in the $Pt/SiW_{11}O_{39}M$-HPB (M=Zn, Co, Ni and Cu) catalytic systems as shown in Figure 1. After 6 h, the amounts of $H_2$ produced are 89.7, 58.6, 39.0 and 28.8 μmol for $SiW_{11}Cu$, $SiW_{11}Ni$, $SiW_{11}Co$ and $SiW_{11}Zn$, respectively (Figure 1). The $H_2$ evolution rates are 150, 98, 65 and 48 μmol h$^{-1}$g$^{-1}$ for $SiW_{11}Cu$, $SiW_{11}Ni$, $SiW_{11}Co$ and $SiW_{11}Zn$, respectively. According to these $H_2$ evolution rates, the order of photocatalytic activity of TMSP-HPBs was as follows: $SiW_{11}Cu > SiW_{11}Ni > SiW_{11}Co > SiW_{11}Zn$, which is in agreement with the visible adsorption spectra of the TMSP-HPB catalyst. It suggests that the nature of the transition metal ions participating in substitution has an influence on the visible adsorption spectra of the corresponding TMSP-HPB catalyst.

Blank experiments (without TMSPs or Zn) were carried out. No hydrogen was detected in 6 h during the blank experiments (Figure 1). Hence, the $H_2$ evolution can be
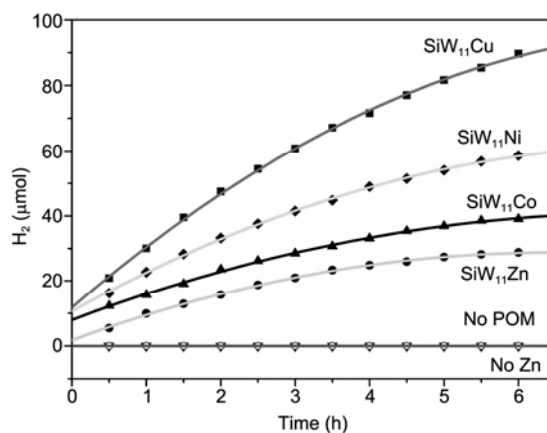


**Figure 1** Time courses of photocatalytic $H_2$ evolution over $SiW_{11}M$ (M= Ni, Co, Cu and Zn) in 50 mL water under visible light irradiation ($\lambda > 420$ nm), $6 \times 10^{-5}$ mol/L catalyst, 2.4 μmol/L Pt; light source, Xe lamp (500 W).

attributed to the intermediate product HPB and related H$^+$ reduction reaction on the Pt nanoparticle surfaces. A feasible mechanism is as follows: firstly, POMs are converted to HPB; secondly, HPB adsorbs visible light to yield its excited-state (HPB*), and HPB* donates the excited electrons at the Pt nanoparticle surfaces to reduce H$^+$ to H atom; at the same time HPB* recovers to POMs.

To explore the stability of the catalysts, recycling studies were performed. There is no difference in IR spectra between the fresh catalyst and the recovered one (Figure S3), which indicates that the recovered catalyst retains the structure of the TMSPs. During the recycling studies, no obvious change of H$_2$ production activity was observed (Figures 2–5), which shows that the catalyst is stable and can be regenerated for repeated use. The observed small decrease in the H$_2$ production can be attributed to catalyst loss during recovering.

## 3  Conclusions

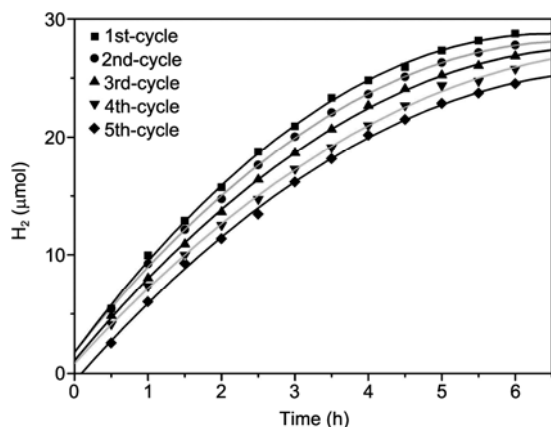In summary, we have studied the visible-light photocatalytic



**Figure 2**  Hydrogen production cycles with recycled catalyst (1–5 cycles) under reaction conditions of $6 \times 10^{-15}$ mol/L catalyst SiW$_{11}$Zn, 2.4 μmol/L Pt in 50 mL water.
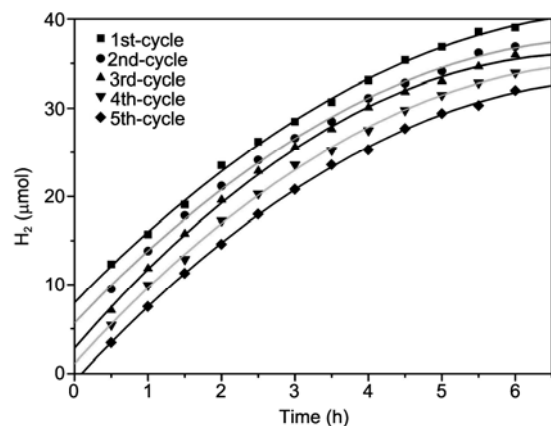


**Figure 3**  Hydrogen production cycles with recycled catalyst (1–5 cycles) under reaction conditions of $6 \times 10^{-5}$ mol/L catalyst SiW$_{11}$Co, 2.4 μmol/L Pt in 50 mL water.
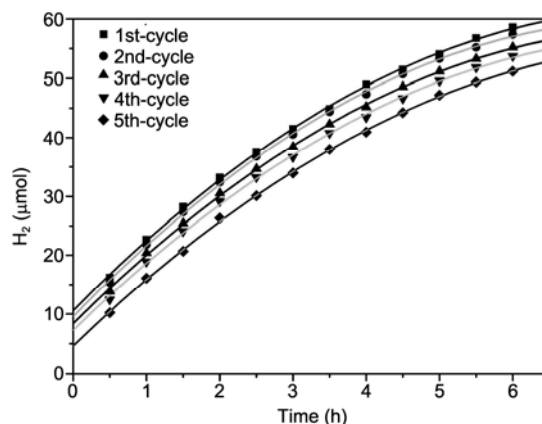


**Figure 4**  Hydrogen production cycles with recycled catalyst (1–5 cycles) under reaction conditions of $6 \times 10^{-5}$ mol/ L catalyst SiW$_{11}$Ni, 2.4 μmol/ L Pt in 50 mL water.
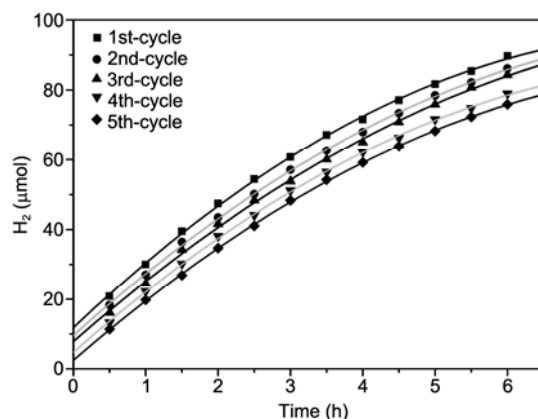


**Figure 5**  Hydrogen production cycles with recycled catalyst (1–5 cycles) under reaction conditions of $6 \times 10^{-5}$ mol/L catalyst SiW$_{11}$Cu, 2.4 μmol/L Pt in 50 mL water.

H$_2$ evolution over a series of transition metal substituted Keggin-structure HPBs of SiW$_{11}$O$_{39}$M (M=Ni, Co, Cu, Zn). The order of photocatalytic activity of these TMSP-HPBs was: SiW$_{11}$Cu > SiW$_{11}$Ni > SiW$_{11}$Co > SiW$_{11}$Zn. These TMSP-HPB catalysts are stable in the present catalytic system; no significant change in the photocatalytic activity was detected even after five cycles. This work reveals the promise of TMSP-HPBs as catalysts for visible light photocatalytic H$_2$ evolution.

1   Lubitz W, Tumas W. Hydrogen: An overview. Chem Rev, 2007, 107: 3900–3903
2   Kudo A, Miseki Y. Heterogeneous photocatalyst materials for water

splitting. Chem Soc Rev, 2009, 38: 253–278

3   Maeda K, Teramura K, Lu D, et al. Catalytic enantioselective α-acylvinyl anion reactions of sliyloxyallenes. Angew Chem Int Ed, 2006, 45: 7806–7809

4   Tessier F, Maillard P, Lee Y G, et al. Zinc germanium oxynitride: Influence of the preparation method on the photocatalytic properties for overall water splitting. J Phys Chem C, 2009, 113: 8526–8531

5   Brown G M, Brunschwig B S, Creutz C, et al. Exicted-state photochemistry in the tris (2,2′-bipyridine) ruthenium(II)—Sulfite system. J Am Chem Soc, 1979, 101: 1298–1300

6   Krishnan C V, Sutin N. Homogeneous catalysis of the photoreduction of water by visible light. 2. Mediation by tris (2,2′-bipyridine) ruthenium(II)-cobalt(II) bipyridine system. J Am Chem Soc, 1981, 103: 2141–2142

7   Fisher J R, Cole-Hamilton D J. Photochemical hydrogen production from ascorbic acid catalysed by tris (2,2′-bipyridyl) ruthenium (II) and hydridotris (triethylphosphine) palladium(II). J Chem Soc, Dalton Trans, 1984, 809–813

8   Krishnan C V, Brunschwig B S, Creutz C, et al. Homogeneous catalysis of the photoreduction of water. 6. Mediation by polypyridine complexes ruthenium(II) and cobalt(II) in alkaline media. J Am Chem Soc, 1985, 107: 2005–2015

9   Goldsmith J I, Hudson W R, Lowry M S, et al. Discovery and high-throughput screening of heteroleptic iridium complexes for photoinduced hydrogen production. J Am Chem Soc, 2005, 127: 7502–7510

10   Du P, Knowles K, Eisenberg R. A homogeneous system for the photogeneration of hydrogen from water based on a platinum (II) terpyridyl acetylide chromophore and a molecular cobalt catalyst. J Am Chem Soc, 2008, 130: 12576–12577

11   Fihri A, Artero V, Razavet M, et al. Cobaloxime-based photocatalytic devices for hydrogen production. Angew Chem Int Ed, 2008, 47: 564–567

12   Fihri A, Artero V, Pereira A, et al. Efficient H$_2$-producing photocatalytic systems based on cyclometalated iridium- and tricarbonyl-rhenium-diimine photosensitizers and cobaloxime catalysts. Dalton Trans, 2008, 5567–5569

13   Na Y, Pan J, Wang M, et al. Intermolecular electron transfer from photogenerated Ru(bpy)$^{3+}$ to [2Fe$_2$S] model complexes of the iron-only hydrogenase active site. Inorg Chem, 2007, 46: 3813–3815

14   Na Y, Wang M, Pan J, et al. Visible light-driven electron transfer and

hydrogen generation catalyzed by bioinspired [2Fe$_2$S] complexes. Inorg Chem, 2008, 47: 2805–2810

15   Okuhara T. Microporous heteropoly compounds and their shape selective catalysis. Appl Catal A, 2003, 256: 213–224

16   Yamase T, Watanabe R. Photoredox chemistry of Keggin dodecatungstoborate [BW$_{12}$O$_{40}$]$^{5-}$ and role of heterogeneous catalysis in hydrogen formation. J Chem Soc, Dalton Trans, 1986, 1669–1675

17   Darwent J R. Photocatalytic hydrogen evolution from alcohols using dodecawolframosilicic acid colloidal platinum. J Chem Soc, Chem Commun, 1982, 798–799

18   Hill C L, Bouchard D A. Catalytic photochemical dehydrogenation of organic substrates by polyoxometalates. J Am Chem Soc, 1985, 107: 5148–5157

19   Ioannidis A, Papaconstantinou E. Photocatalytic generation of hydrogen by 1:12 heteropolytungstates with concomitant oxidation of organic compounds. Inorg Chem, 1985, 24: 439–441

20   Yamase T, Takabayashi N, Kaji M. Solution photochemistry of tetrakis(tetrabutylammonium) decatungstate(VI) and catalytic hydrogen evolution from alcohols. J Chem Soc, Dalton Trans, 1984, 793–799

21   Yamase T, Cao X O, Yazaki S. Structure of double Keggin-Ti/W-mixed polyanion [(A-β-GeTi$_3$W$_9$O$_{37}$)$_2$O$_3$]$^{14-}$ and multielectron-transfer-based photocatalyic H$_2$-generation. J Mol Catal A: Chem, 2007, 262: 119–127

22   Bi L, Kortz U, Keita B, et al. The ruthenium (II)-supported heteropolytungstates [Ru(dmso)$_3$(H$_2$O)XW$_{11}$O$_{39}$]$^{6-}$(X=Ge, Si). Dalton Trans, 2004, 3184–3190

23   Briand L E, Baronetti G T, Thomas H J. The state of the art on Wells-Dawson heteropoly-compounds: A review of their properties and applications. Appl Catal A, 2003, 256: 37–50

24   Yoon M, Chang J A, Kim Y, et al. Heteropoly acid-incorporated TiO$_2$ colloids as novel photocatalytic systems resembling the photosynthetic reaction center. J Phys Chem B, 2001, 105: 2539–2545

25   Chatti R, Rayalu S S, Dubey N, et al. Solar-based photoreduction of methyl orange using zeolite supported photocatalytic materials. Energy Mater Sol Cells, 2007, 91: 180–190

26   Fu N, Lu G X. Graft of lacunary Wells–Dawson heteropoly blue on the surface of TiO$_2$ and its photocatalytic activity under visible light. Chem Commun, 2009, 3591–3593

27   Weakley T J R, Malik S A. Heteropolyanions containing two different heteroatoms-1. J Inorg Nucl Chem, 1967, 29: 2935–2944

## Supporting Information

**Figure S1**   The UV-visible spectra of the HPBs of SiW$_{11}$Cu (a), SiW$_{11}$Ni (b), SiW$_{11}$ Co (c), and SiW$_{11}$Zn (d).

**Figure S2**   The visible adsorption spectra (400–800 nm) of TMSPs. (A) SiW$_{11}$Cu (a) and HPB of SiW$_{11}$Cu (b); (B) SiW$_{11}$Ni (a) and HPB of SiW$_{11}$Ni (b); (C) SiW$_{11}$Co (a) and HPB of SiW$_{11}$Co (b); (D) SiW$_{11}$Zn (a) and HPB of SiW$_{11}$Zn (b).

**Figure S3**   (A) FT-IR spectra of fresh SiW$_{11}$Co (a) and reused SiW$_{11}$Co (b); (B) fresh SiW$_{11}$Ni (a) and reused SiW$_{11}$Ni (b); (C) fresh SiW$_{11}$Cu (a) and reused SiW$_{11}$Cu (b); (D) fresh SiW$_{11}$Zn (a) and reused SiW$_{11}$Zn (b) in the range of 4000–400 cm$^{-1}$.

The supporting information is available online at csb.scichina.com and www.springerlink.com. The supporting materials are published as submitted, without typesetting or editing. The responsibility for scientific accuracy and content remains entirely with the authors.